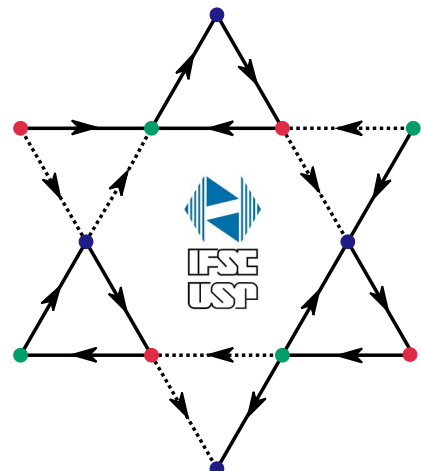


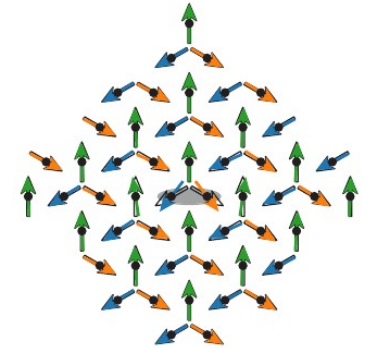
Noncoplanar magnetism and chiral spin liquids on the Kagome Lattice



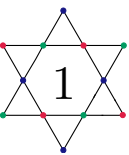
João Augusto Sobral
University of São Paulo, IFSC

University of Innsbruck
Wednesday, 11/May/2022

Main ref: (arXiv:2112.03327)



Novel Quantum Materials
Prof. Eric C. Andrade's
group (IFSC/USP)

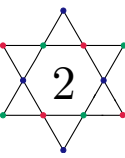


Acknowledgements



- ✉ Prof. Mathias S. Scheurer.
- ✉ Prof. Eric de Castro e Andrade.
- ✉ Prof. Rodrigo G. Pereira e Fabrizio G. Oliviero.
- ✉ Vitor Dantas Meireles.
- ✉ CAPES - Finance Code 001, via Grant No. 88887.474253/2020-00.





Outline

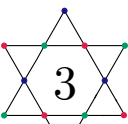
0 Motivation and Methodology

- Frustrated magnetism on the Kagome lattice
- Ordered phases and classical phase diagrams
- Parton Construction and Variational Monte Carlo (VMC)
- Example: Quantum spin liquids on the kagome lattice

1 Noncoplanar ordered phases on the kagome lattice

2 Gapless chiral spin liquid on the kagome lattice

Mott Insulators, Frustrated Magnetism and Quantum Spin Liquids (QSL)



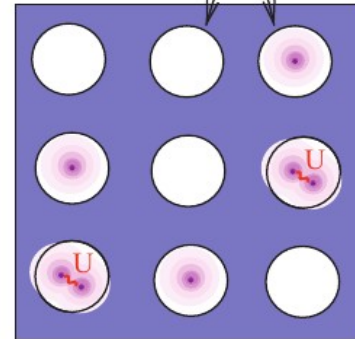
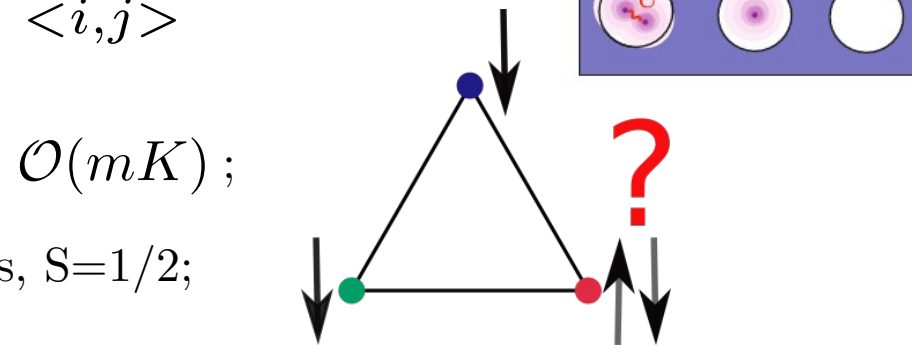
$$H = -t \sum_{j, \hat{a}, \sigma} c_{j+\hat{a}\sigma}^\dagger c_{j\sigma} + \epsilon \sum_{j\sigma} c_{j\sigma}^\dagger c_{j\sigma} + U \sum_j n_{j\uparrow} n_{j\downarrow}$$

$\rightarrow U/t \gg 1 \rightarrow \mathcal{H} = J \sum_{\langle i,j \rangle} \mathbf{S}_i \cdot \mathbf{S}_j$

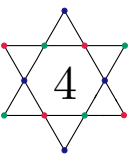
Th: P. Coleman, Introduction to many-body physics (2015)

- ◊ Absence of magnetic order up to $T \sim \mathcal{O}(mK)$;
- ◊ Fractionalized excitations, e.g.: Spinons, $S=1/2$;
- ◊ Gapless (emergent fermions coupled to gauge fields) and gapped (topological ground state degeneracy).

Th: Anderson, Mater. Res. Bull. **8**, 153 (1973) | Savary, Balents, Rep Prog. Phys. 2017 Anderson, Science **235**, 1196 (1987)



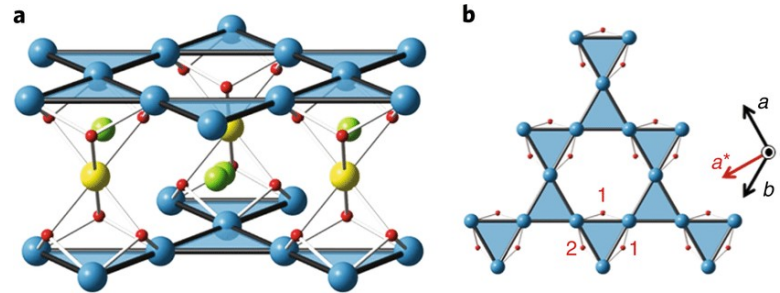
Frustrated magnetism on the Kagome lattice



Herbertsmithite



Exp: P. Khuntia, *et al*, Nat. Phys. **16**, 469–474 (2020).



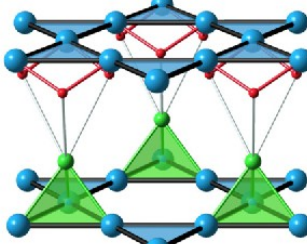
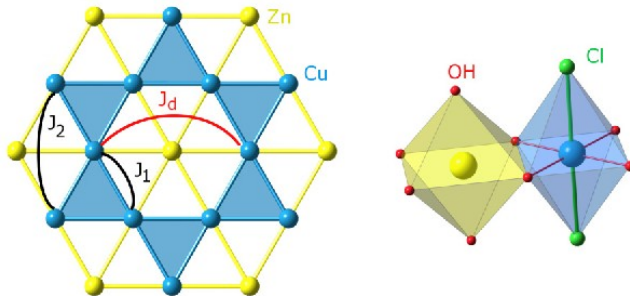
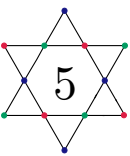
Kapellasite



Exp: E. Kermarrec, *et al*,
Phys. Rev. B **90**, 205103
(2014)

$$\text{Cu}_3\text{Zn}(\text{OH})_6\text{Cl}_2$$

Kapellasite: a candidate for a GQSL?

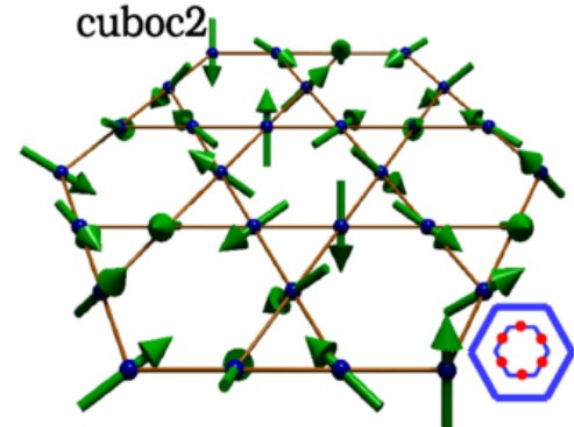


Weak O-H-Cl coupling between Kagome planes.

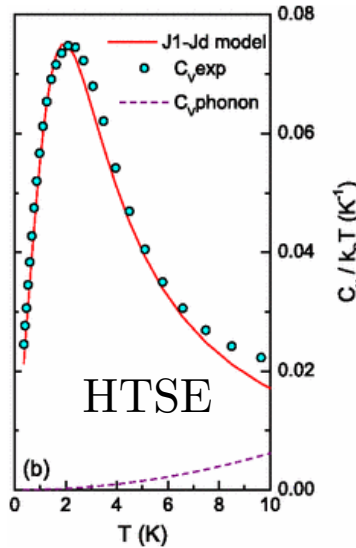
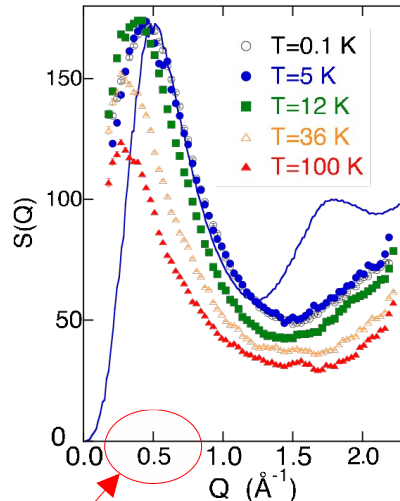
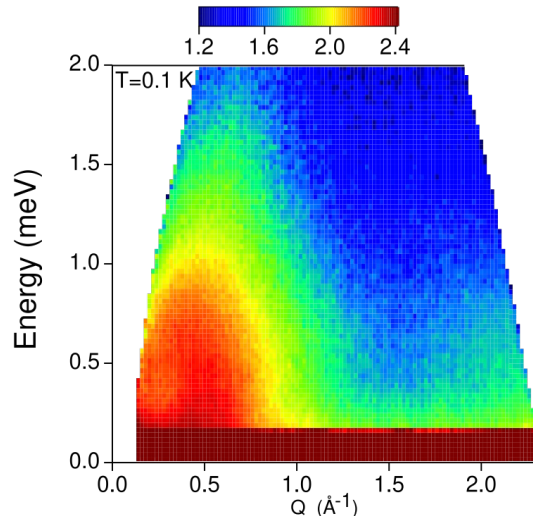
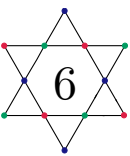
- ◊ Polymorphous to Herberthsmithite ($U(1)$ QSL e $J_1 > 0$);
- ◊ Gapless spin liquid ($\Delta \lesssim 10^{-3} J_1$);
- ◊ Short-range magnetic correlations of cuboc-2 type
- ◊ up to $T = 20$ mK.

$$\mathbf{S}(\mathbf{r}_i) \cdot [\mathbf{S}(\mathbf{r}_j) \times \mathbf{S}(\mathbf{r}_k)]$$

Exp: Fåk, Phys. Rev. Lett. 109, 037208T (2012)

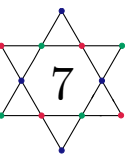


Kapellasite: a candidate for a GQSL?



- ◊ Bragg peaks (cuboc-2);
- ◊ Continuum of excitations (spinons);
- ◊ Curie-Weiss Law ($\chi \propto 1/(T - \Theta_n)$), $\Theta_n = 9.5 \pm 1 K$)

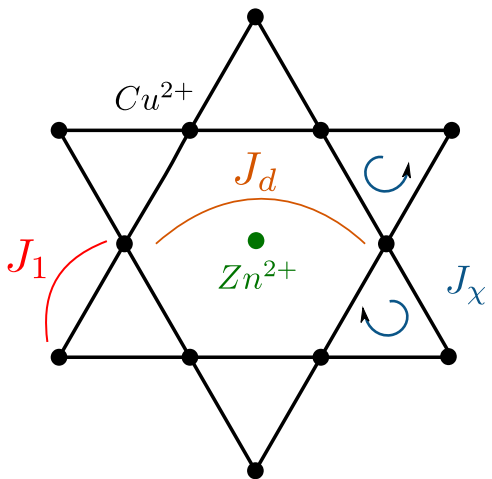
Exp: Fåk *et al*, Phys. Rev. Lett.
109, 037208T (2012)



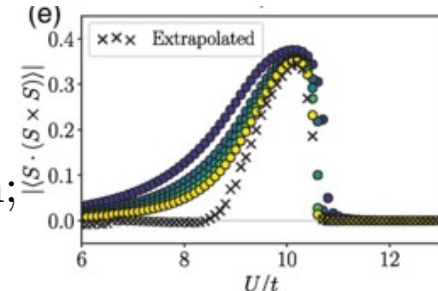
Modified Heisenberg model $J_1 - J_d - J_\chi$

$$H = J_1 \sum_{\langle i,j \rangle} \mathbf{S}(\mathbf{r}_i) \cdot \mathbf{S}(\mathbf{r}_j) + J_d \sum_{ij \in \Delta} \mathbf{S}(\mathbf{r}_i) \cdot \mathbf{S}(\mathbf{r}_j) + \\ + J_\chi \sum_{ijk \in \Delta} \mathbf{S}(\mathbf{r}_i) \cdot [\mathbf{S}(\mathbf{r}_j) \times \mathbf{S}(\mathbf{r}_k)] - J_\chi \sum_{ijk \in \nabla} \mathbf{S}(\mathbf{r}_i) \cdot [\mathbf{S}(\mathbf{r}_j) \times \mathbf{S}(\mathbf{r}_k)],$$

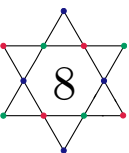
$J_1 < 0$ (FM), $J_d > 0$ (AFM) e $J_\chi > 0$



- ◊ Staggered chirality;
- ◊ Noncoplanar phases and CSLs;
- ◊ Amplified near the Mott transition;
- ◊ Floquet engineering.



Th: Claassen *et al*, Nat. Com. v.8, 1192 (2017) | Quito *et al*, Phys. Rev. Lett. 126, 177201 (2021) | Cookmeyer *et al* Phys. Rev. Lett. 127, 087201 (2021) | Szasz *et al* Phys. Rev. X 10, 021042 (2020)



Classical Phases: Gradient descent and SSSF (\mathbf{S} classical)

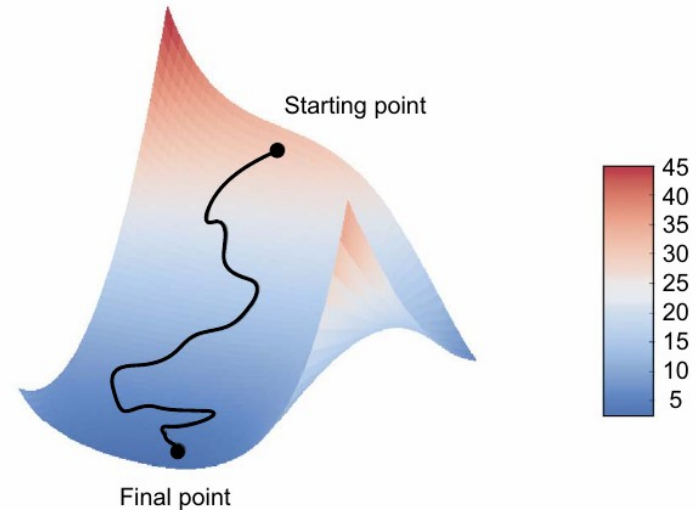
$$\mathcal{H}_{GD} = \sum_i \mathbf{S}_i \cdot \mathbf{h}_i$$

$$\mathbf{h}_i = J_1 \sum_j \mathbf{S}_j + J_d \sum_{j \in} \mathbf{S}_j + J_\chi \sum_{j,k \in \Delta \nabla} (\mathbf{S}_j \times \mathbf{S}_k)$$

$$-\nabla_i \mathcal{H}_{GD} (\mathbf{S}_i) \parallel \mathbf{h}_i$$

$$\nabla_i \mathcal{H}_{GD} = \frac{\partial \mathcal{H}_{GD}}{\partial S_i^x} \hat{x} + \frac{\partial \mathcal{H}_{GD}}{\partial S_i^y} \hat{y} + \frac{\partial \mathcal{H}_{GD}}{\partial S_i^z} \hat{z} = \mathbf{h}_i$$

$$\mathbf{S}_{i+1} = (1 - \gamma) \mathbf{S}_i - \gamma \nabla_i \mathcal{H} (\mathbf{S}_i)$$



Chollet, Deep Learning with Python (2021)

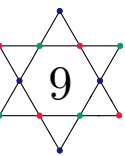
^{*} Accessible experimentally through inelastic neutron scattering data (INS).

SSSF

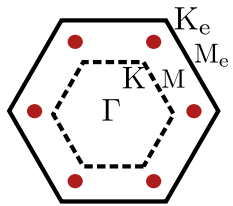
$$\mathbf{S}_\mathbf{k} = \frac{1}{\sqrt{N}} \sum_r e^{-i \mathbf{r} \cdot \mathbf{k}} \mathbf{S}_r$$

$$\mathcal{S}(m_1, m_2) = \mathbf{S}_\mathbf{k} \cdot \mathbf{S}_{-\mathbf{k}} = |\mathbf{S}_\mathbf{k}|^2$$

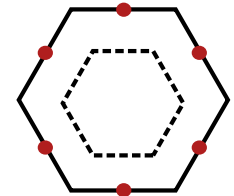
Classical Phases: Gradient descent and SSSF (S classical)



cuboc-1

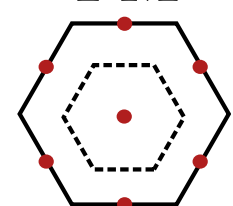


$$Q = 0 \times 0$$

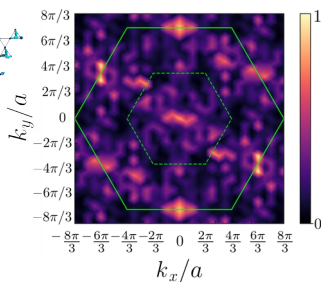
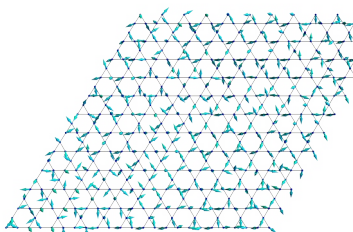


cuboc-2

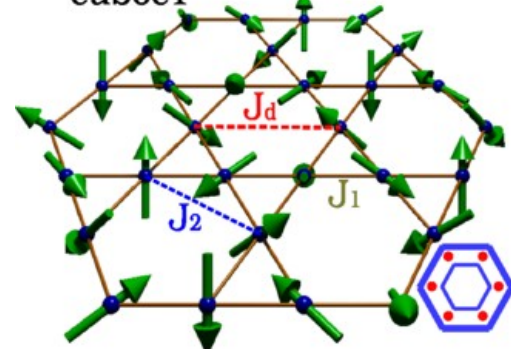
FM



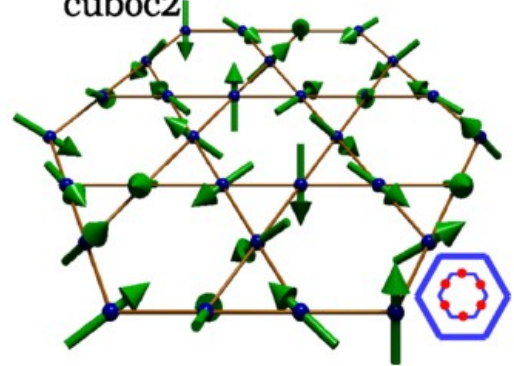
$$Q = \sqrt{3} \times \sqrt{3}$$



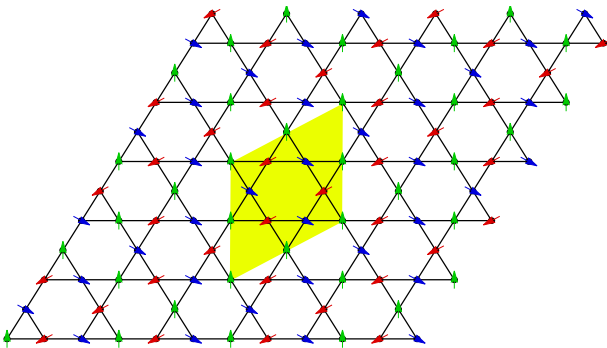
cuboc1



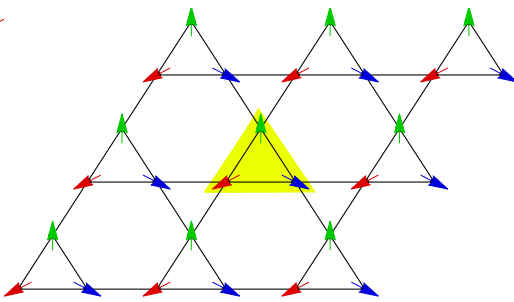
cuboc2



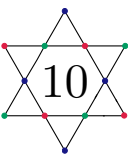
$$Q = \sqrt{3} \times \sqrt{3}$$



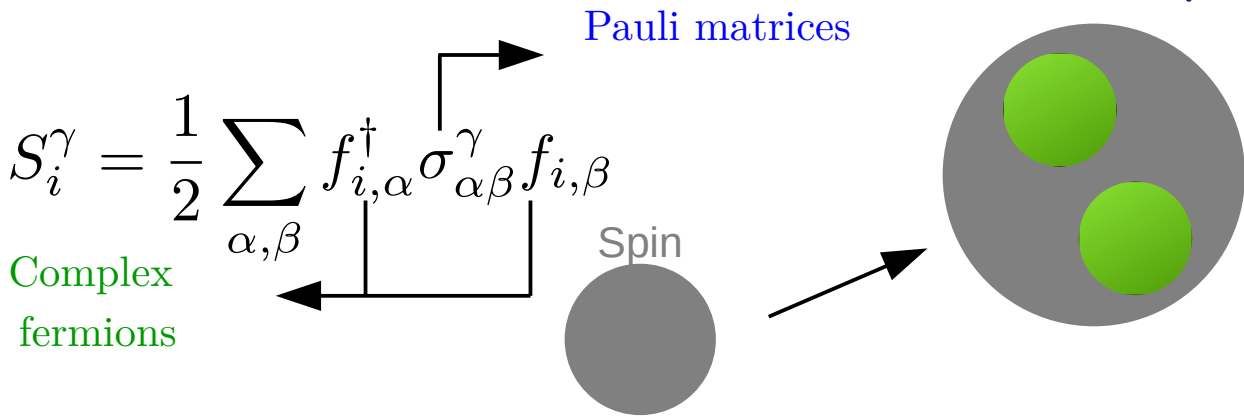
$$Q = 0 \times 0$$



Parton Construction and Gutzwiller Projection ($S = 1/2$)



Abrikosov
Fermions



$$\hat{S}_i^+ = f_{i\uparrow}^\dagger f_{i\downarrow}, \hat{S}_i^- = f_{i\downarrow}^\dagger f_{i\uparrow} \quad e \quad \hat{S}_i^z = \frac{1}{2} (n_{i\uparrow} - n_{i\downarrow}) \quad \text{Single-occupancy constraint (local)}$$

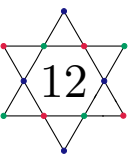
MFT decoupling

$$\chi_{ij} = f_{i\uparrow}^\dagger f_{j\uparrow} + f_{i\downarrow}^\dagger f_{j\downarrow}$$

$$H_{MF} \Psi_{MF} = E \Psi_{MF}$$

$$n_{i\uparrow} + n_{i\downarrow} = 1$$

Parton Construction and Gutzwiller Projection



◊ Ansatz described by a Slater determinant for a singlet state ($S_{tot}=0$), with spin $\frac{1}{2}$ excitations.

◊ The occupancy can be imposed **exactly** through Variational Monte Carlo or MPS, by using the **Gutzwiller projection**:

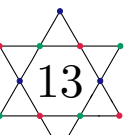
$$|\psi\rangle = \hat{P}_G |\psi_{MF}\rangle \quad \hat{P}_G = \prod_i (2 - n_i) n_i \quad n_i = \sum_\alpha f_{i,\alpha}^\dagger f_{i,\alpha}$$

$$|\psi_{Slater}\rangle = \begin{array}{c} \text{Diagram of a 4x4 grid of red circles with arrows, representing a Slater determinant state.} \end{array} + \begin{array}{c} \text{Diagram of a 4x4 grid with two red circles removed from the second column, representing a projected state.} \end{array} + \begin{array}{c} \text{Diagram of a 4x4 grid with one red circle removed from the second column, representing another projected state.} \end{array} \dots$$

$$\hat{P}_G |\psi_{Slater}\rangle = \begin{array}{c} \text{Diagram of a 4x4 grid of red circles with arrows, representing the original Slater state.} \end{array} + 0 + \begin{array}{c} \text{Diagram of a 4x4 grid with one red circle removed from the second column, representing the Gutzwiller-projected state.} \end{array} \dots$$

Gros, Ann. Phys. **189**, 53 (1989) /
Zou, Y., et al Rev. Mod. Phys. **89**, 025003 (2017). / Gutzwiller, M.,
Phys. Rev. A **137**, A1726 (1964)

Parton construction and VMC



Configurations

$$\langle \mathcal{O} \rangle = \frac{\langle \psi | \mathcal{O} | \psi \rangle}{\langle \psi | \psi \rangle} = \sum_{\alpha \beta} \langle \alpha | \mathcal{O} | \beta \rangle \frac{\langle \psi | \alpha \rangle \langle \beta | \psi \rangle}{\langle \psi | \psi \rangle}.$$

$$\langle \mathcal{O} \rangle = \sum_{\alpha} \left(\sum_{\beta} \langle \alpha | \mathcal{O} | \beta \rangle \frac{\langle \beta | \psi \rangle}{\langle \alpha | \psi \rangle} \right) \frac{|\langle \alpha | \psi \rangle|^2}{\langle \psi | \psi \rangle} = \sum_{\alpha} f(\alpha) p(\alpha)$$

$$f(\alpha) = \left(\sum_{\beta} \langle \alpha | \mathcal{O} | \beta \rangle \frac{\langle \beta | \psi \rangle}{\langle \alpha | \psi \rangle} \right) \rightarrow \text{Statistical average of local operator}$$

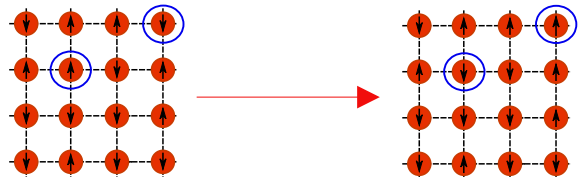
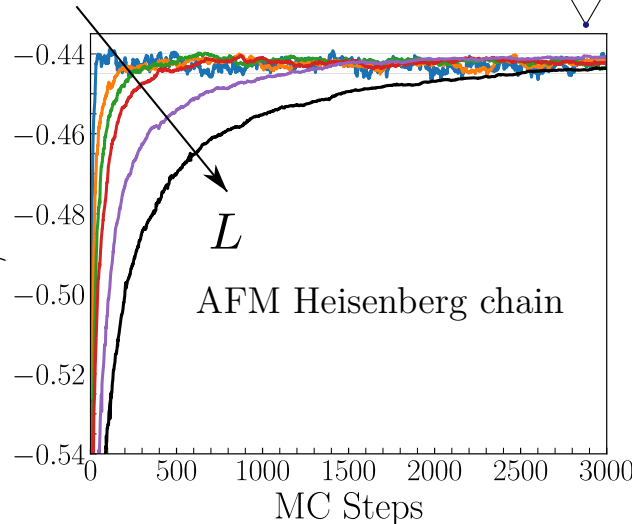
$$p(\alpha) = \frac{|\langle \alpha | \psi \rangle|^2}{\langle \psi | \psi \rangle} \geq 0$$

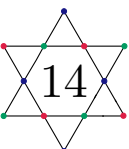
Probability distribution

$$\sum_{\alpha} p(\alpha) = 1.$$

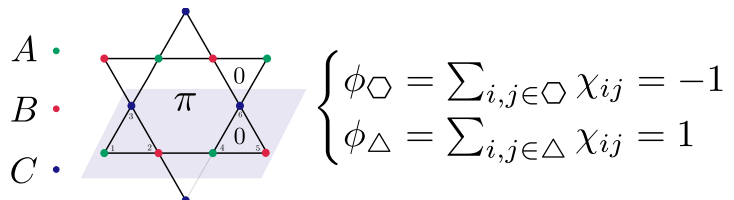
Markov Chain -> Equilibrium

$$T(\alpha \rightarrow \alpha') = \min \left[1, \frac{p(\alpha')}{p(\alpha)} \right] = \begin{cases} \frac{p(\alpha')}{p(\alpha)} & , \frac{p(\alpha')}{p(\alpha)} < 1 \\ 1 & , \frac{p(\alpha')}{p(\alpha)} > 1 \end{cases},$$

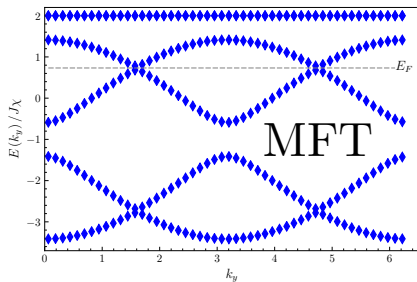




QSLs on the Kagome lattice (Heis. model J_1)



- ◊ CSL $\chi_{i,j} \rightarrow \bar{\chi}_{i,j} e^{-ia_{i,j}}$
- ◊ Uniform RVB with spinon Fermi surface.
- ◊ U(1) Dirac QSL (Stable)?



Herbertsmithite

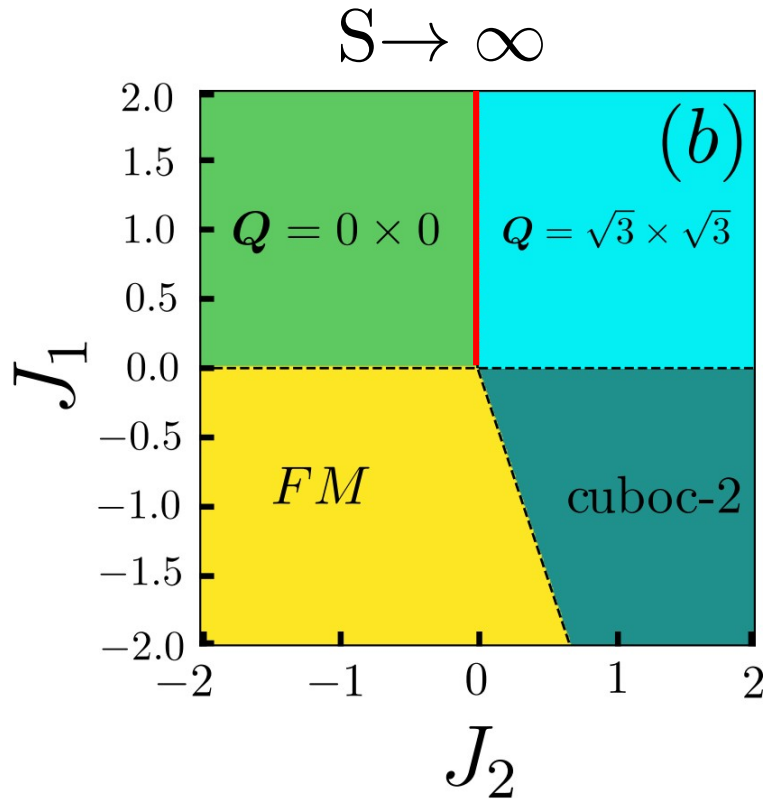
$$H = J_1 \sum_{\langle i,j \rangle} \mathbf{S}(\mathbf{r}_i) \cdot \mathbf{S}(\mathbf{r}_j)$$

Spin liquid	$8 \times 8 \times 3$ lattice	$12 \times 12 \times 3$ lattice
SL-[$\frac{\pi}{2}, 0$]	-0.4010(1)	-0.4010(1)
SL-[$\pm \frac{\pi}{2}, 0$]	-0.3907(1)	-0.3910(1)
SL-[$\frac{\pi}{2}, \pi$]	-0.3814(1)	-0.3822(1)
SL-[0, 0]	-0.4115(1)	-0.4121(1)
SL-[0, π]	-0.42866(2)	-0.42863(2)

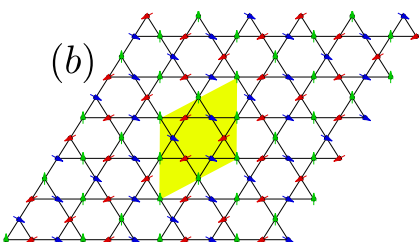
Method	Energy per site
Exact diagonalization [11]	-0.43
Coupled cluster method [14]	-0.4252
Spin-wave variational method [15]	-0.419

M. B. Hastings, Phys. Rev. B 63, 014413 (2000) | Y. Ran, M. Hermele, P. A. Lee, and X.-G. Wen, Phys. Rev. Lett. 98, 117205 (2007). | Y.-C. He, M. P. Zaletel, M. Oshikawa, and F. Pollmann, Phys. Rev. X 7, 031020 (2017)

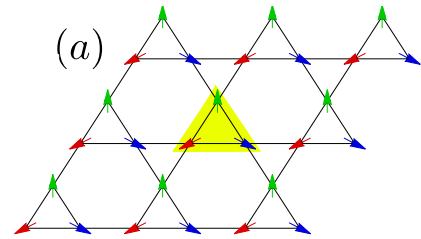
QSLs on the Kagome lattice (Heis. model J_1 - J_2)



$$H = J_1 \sum_{\langle i,j \rangle} \mathbf{S}(\mathbf{r}_i) \cdot \mathbf{S}(\mathbf{r}_j) + J_2 \sum_{\langle\langle i,j \rangle\rangle} \mathbf{S}(\mathbf{r}_i) \cdot \mathbf{S}(\mathbf{r}_j)$$

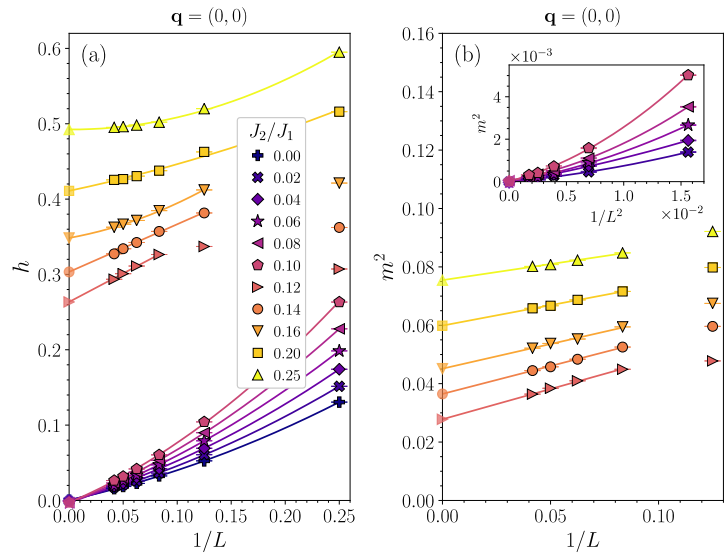
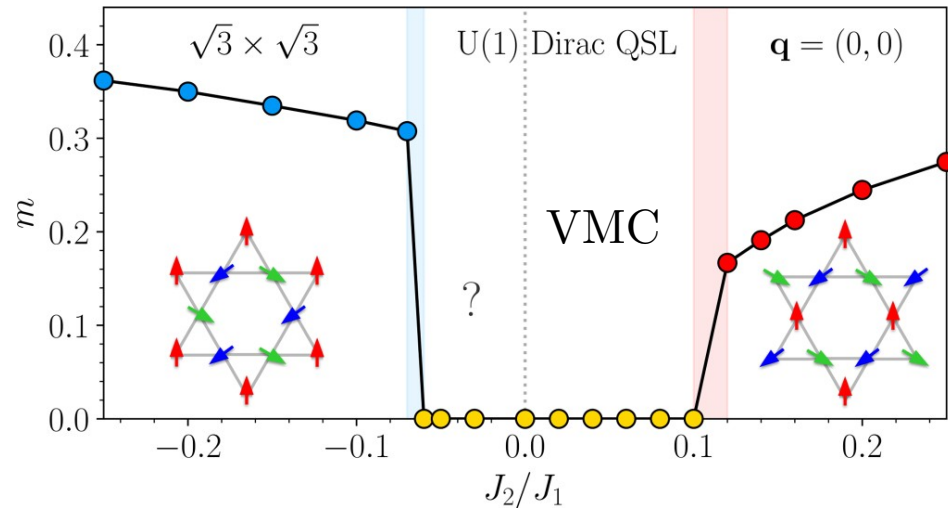
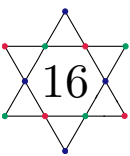


$$Q = \sqrt{3} \times \sqrt{3}$$



$$Q = 0 \times 0$$

QSLs on the Kagome lattice (Heis. model J_1 - J_2)



$$H_{MFT} = \sum_{\langle i,j \rangle, \alpha} \chi_{ij} f_{i\alpha}^\dagger f_{j\alpha} + h \sum_i \mathbf{m}_i \cdot \mathbf{S}_i$$

$$m^2 = \lim_{|i-j| \rightarrow \infty} \langle \mathbf{S}_i \cdot \mathbf{S}_j \rangle$$

SDW

Francesco Ferrari, et al.
Phys. Rev. B 104, 144406
(2021) | Iaconis, SciPost
Phys. 4, 003 (2018)

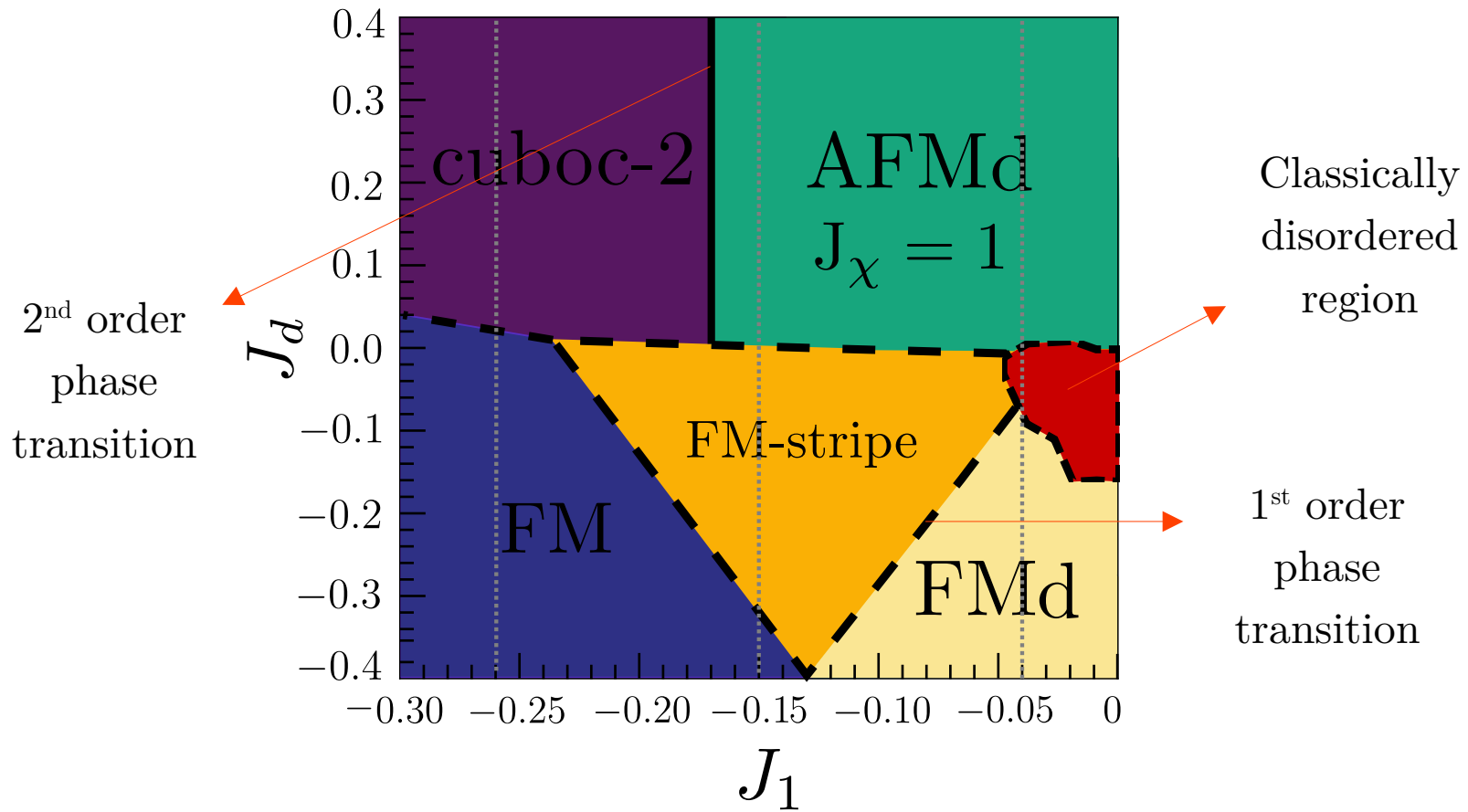


Noncoplanar ordered phases on the
Kagome lattice



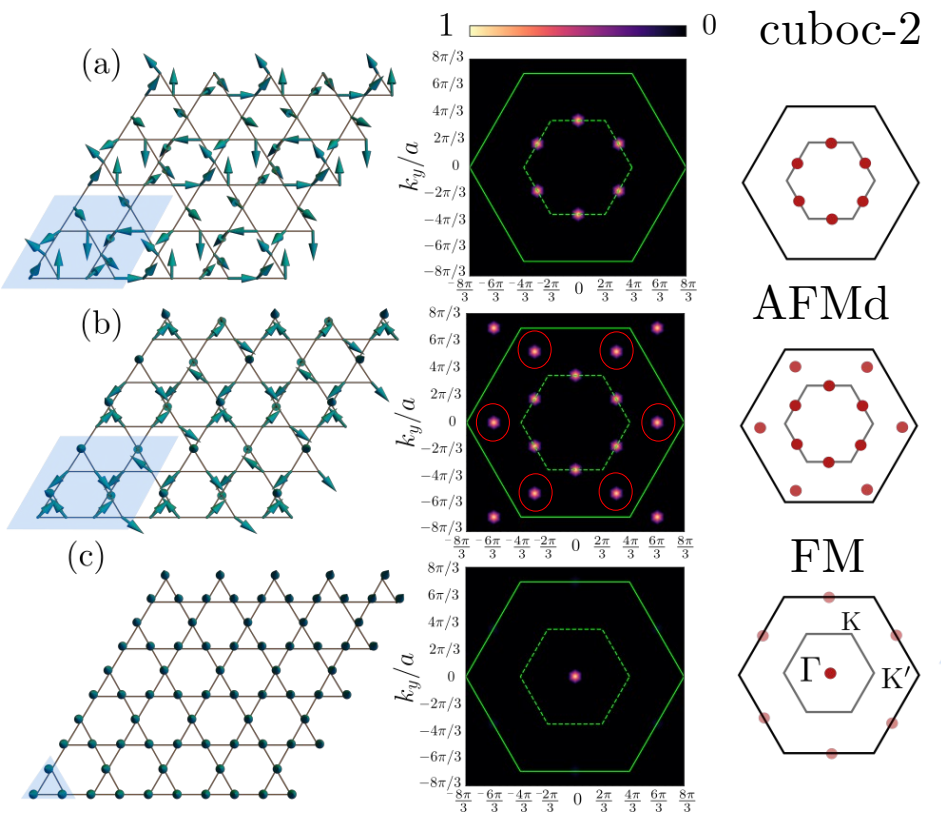
Gapless chiral spin liquid on the Kagome
lattice

Classical phase diagram for the $J_1 - J_d - J_\chi$ model

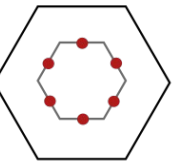


Static spin structure factor (SSSF) and ordered phases

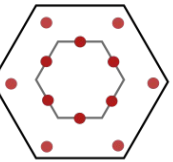
18



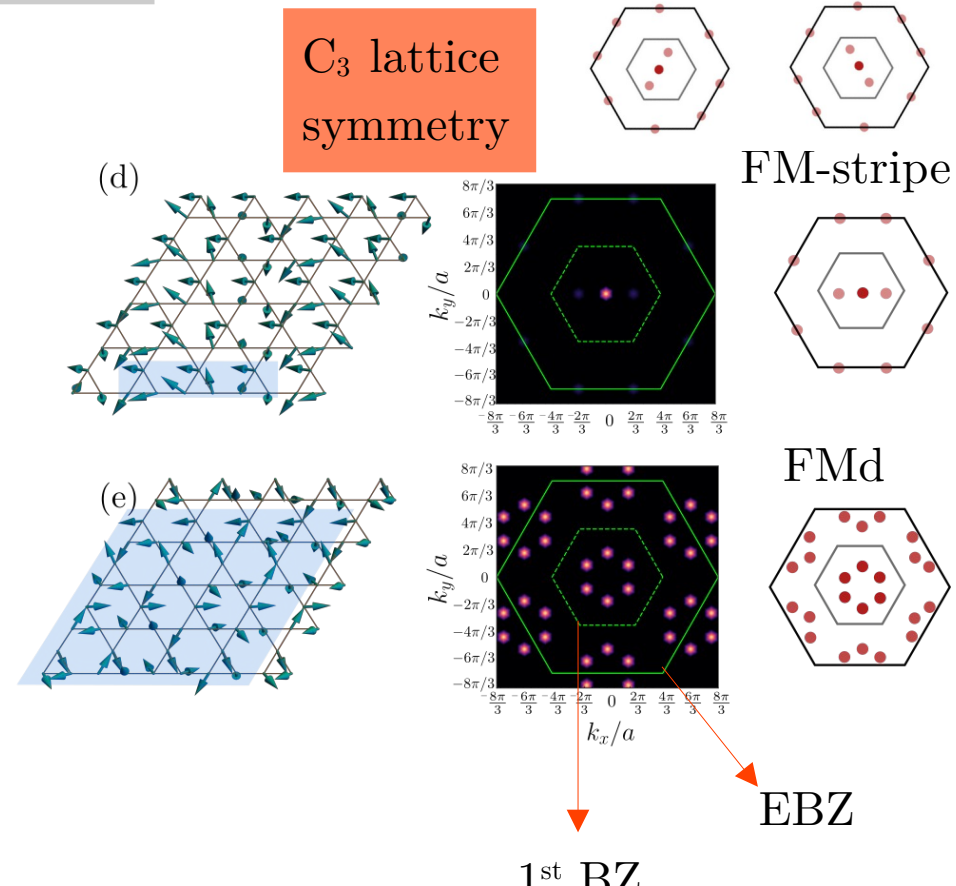
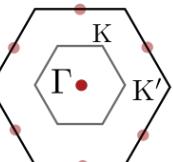
cuboc-2



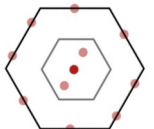
AFMd



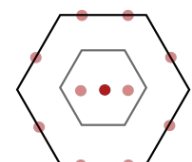
FM



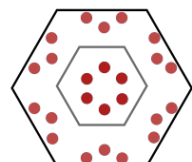
C₃ lattice
symmetry

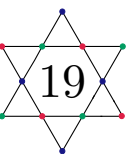


FM-stripe

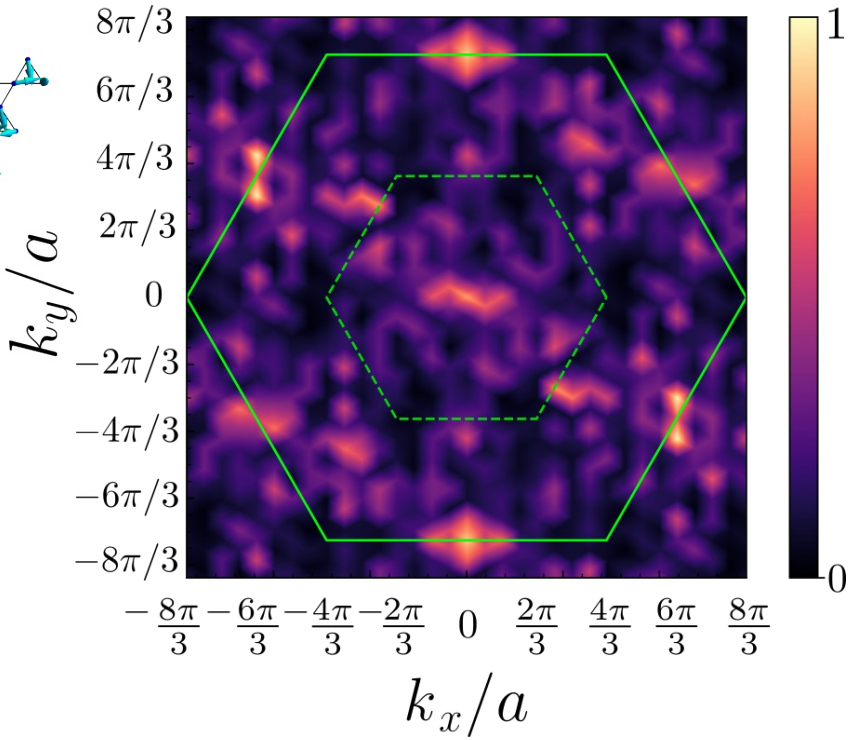
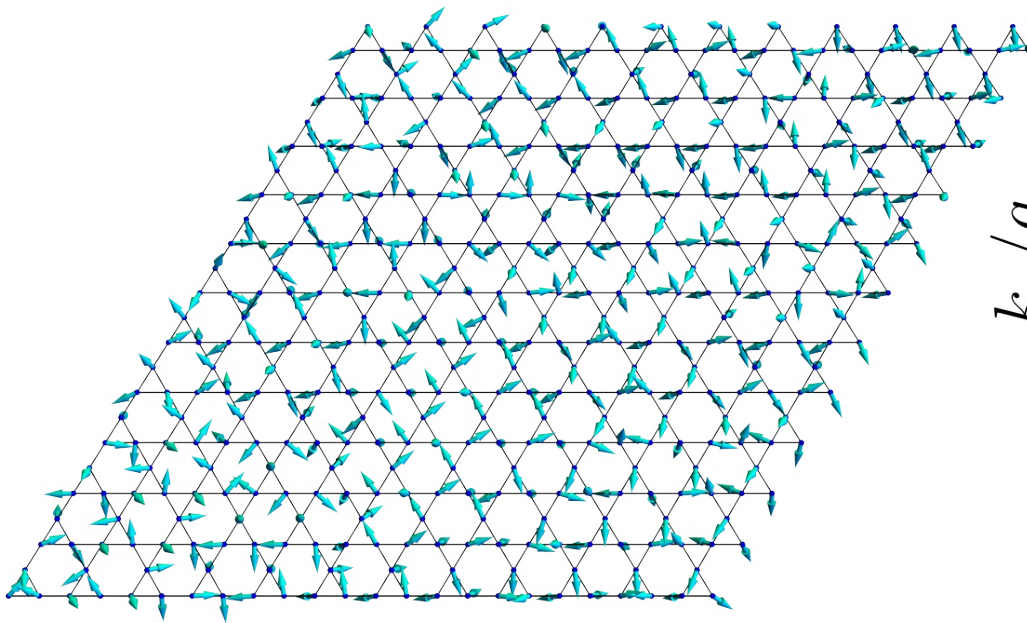


FMD

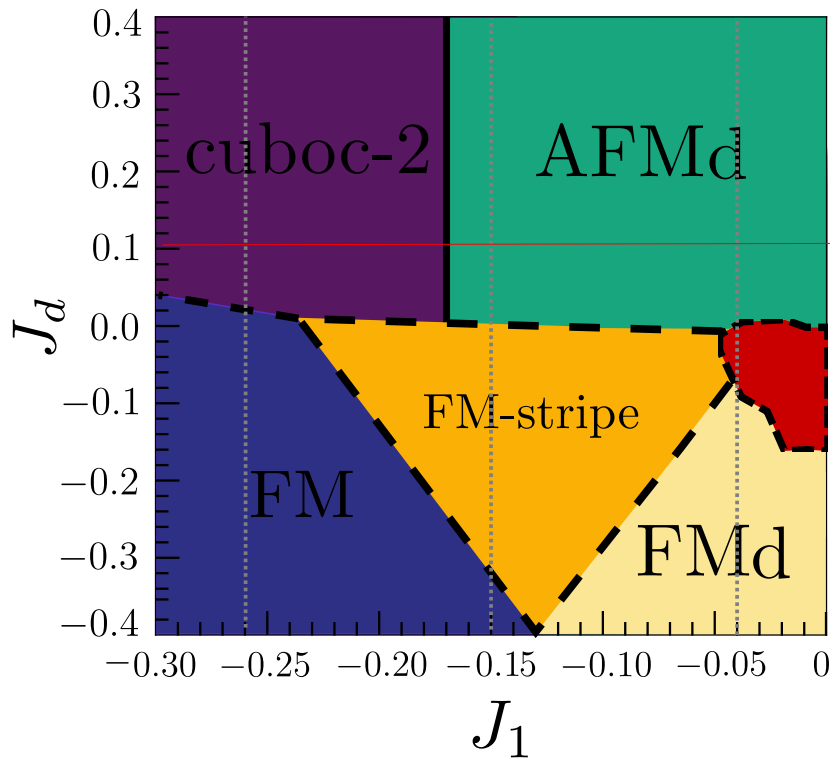
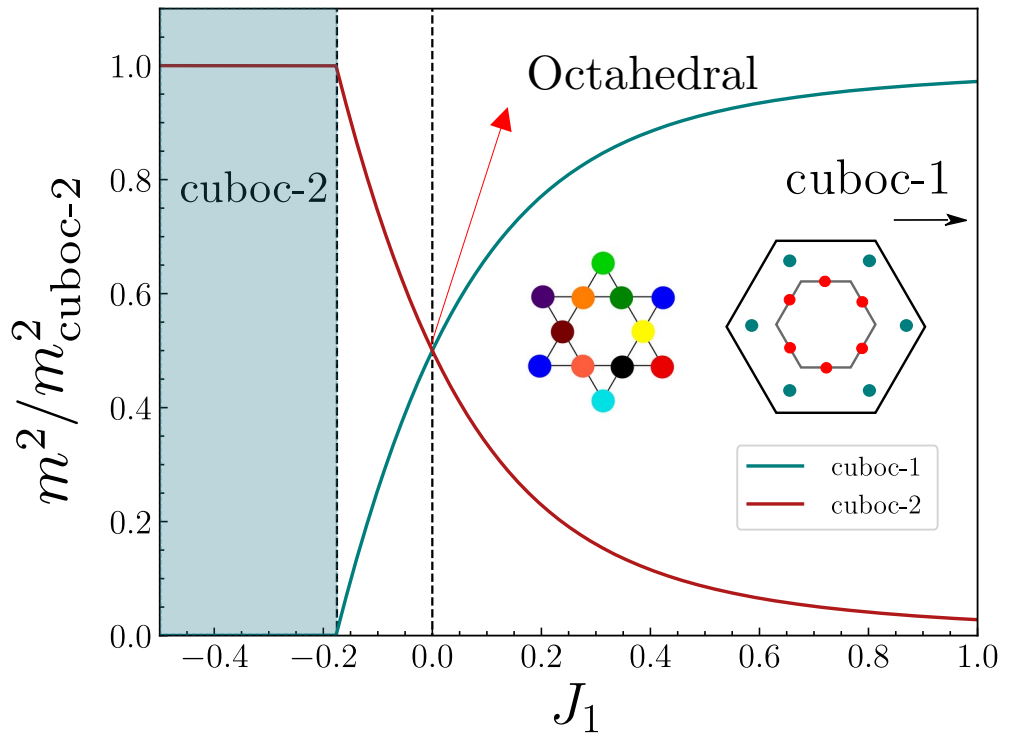
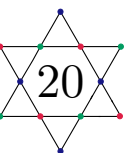




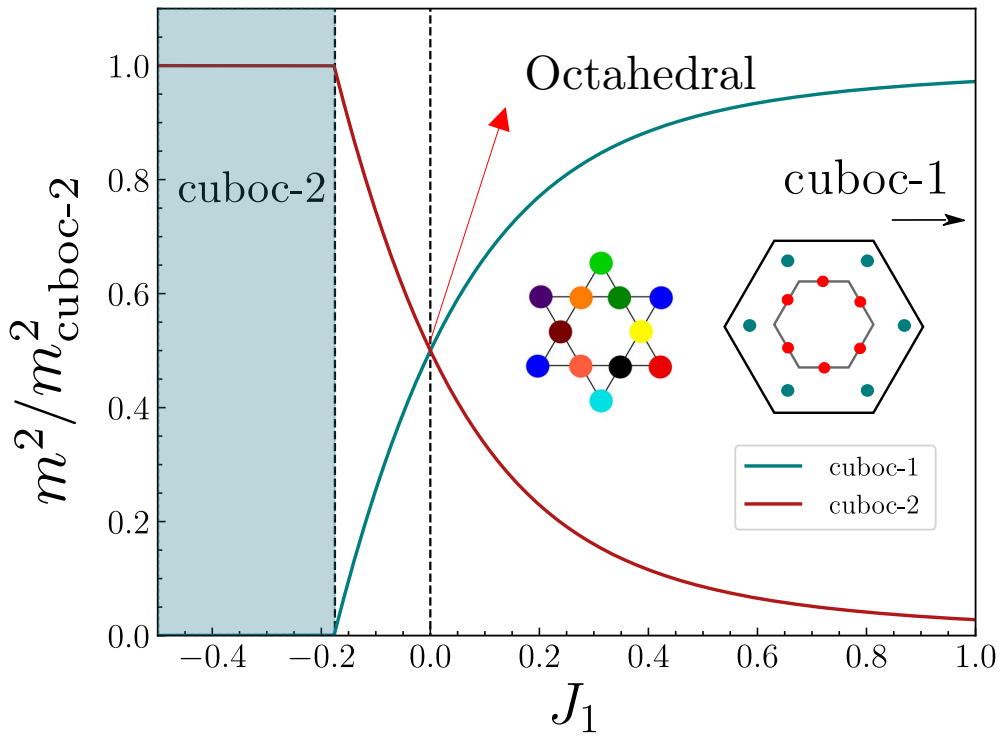
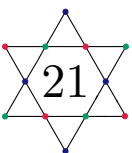
Classically disordered region



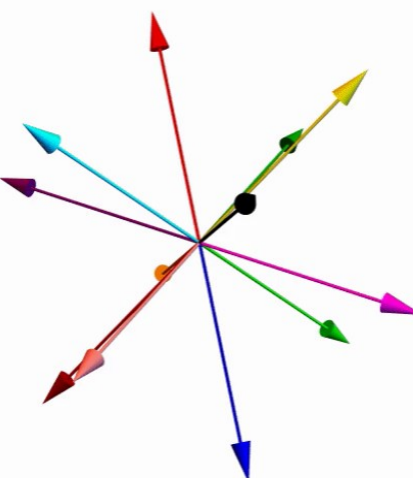
Cuboc-2 and cuboc-1 phase transition (AFMd)



Cuboc-2 and cuboc-1 phase transition (AFMd)



$J_1 = -0.2343$





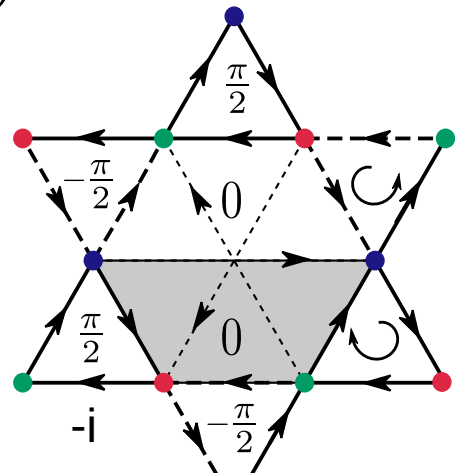
Noncoplanar ordered phases on the kagome lattice



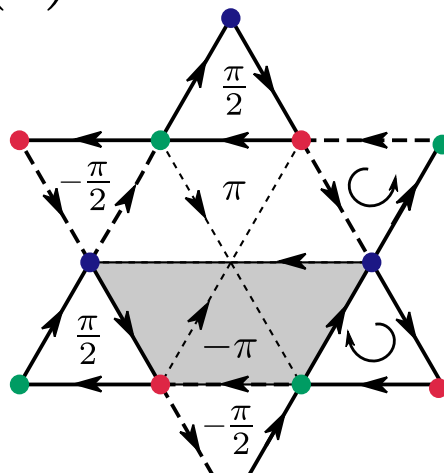
Gapless chiral spin liquid on the kagome lattice

Parton mean-field theory: ansatz $[\pm\pi/2, 0]$

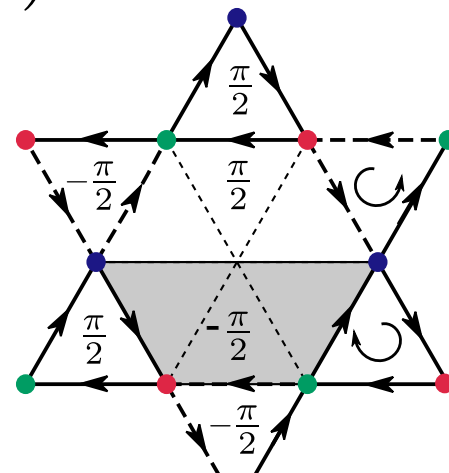
(a) Case I



(b) Case II



(c) Case III





Parton mean-field theory

$$S_i^\gamma = \frac{1}{2} \sum_{\alpha, \beta} f_{i,\alpha}^\dagger \sigma_{\alpha\beta}^\gamma f_{i,\beta}$$

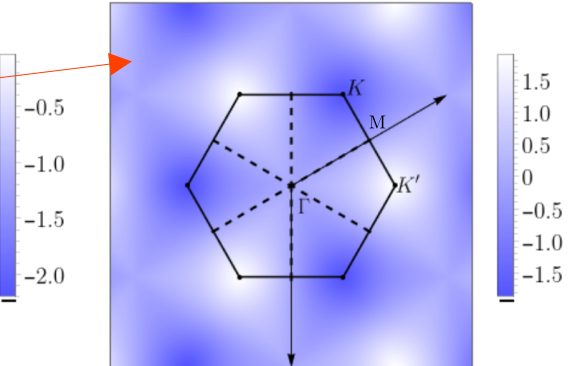
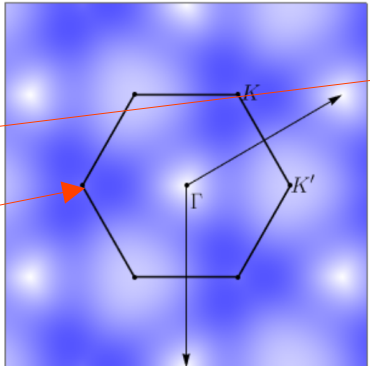
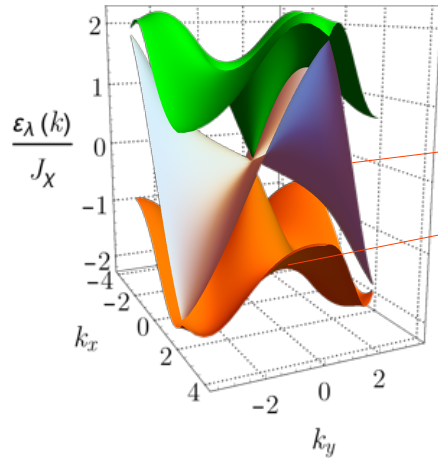
MFT parameters

$$\kappa_1 = \frac{3}{8} J_\chi \chi_1^2 - J_1 \chi_1, \quad \kappa_d = J_d \chi_d$$

- ◊ Energetic favoring for Case II;
- ◊ Nodal lines (dashed lines);
- ◊ Dirac Cones in Γ .

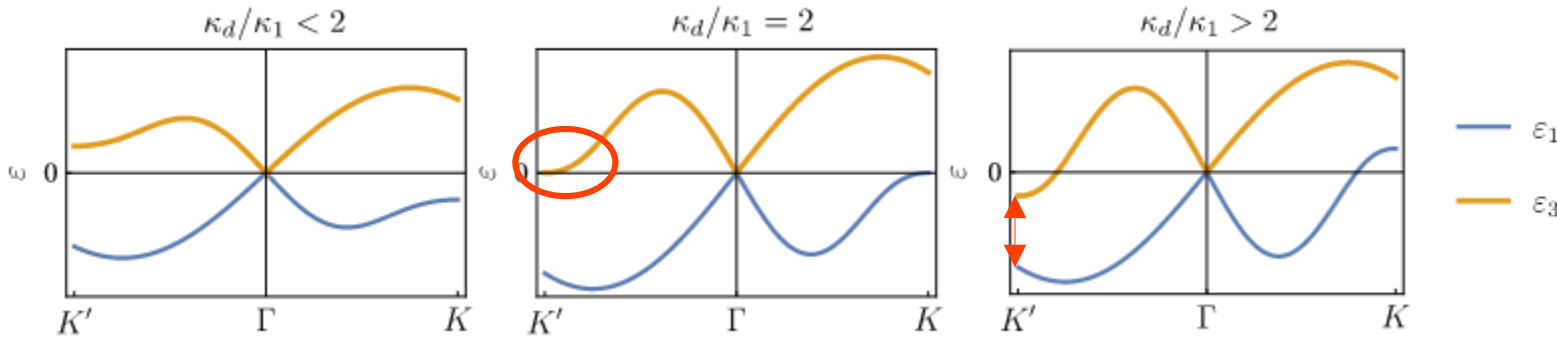
Majorana, J_x only

Bauer et al, Phys. Rev. B 99, 035155 (2019)





Parton mean-field theory (Instabilities)



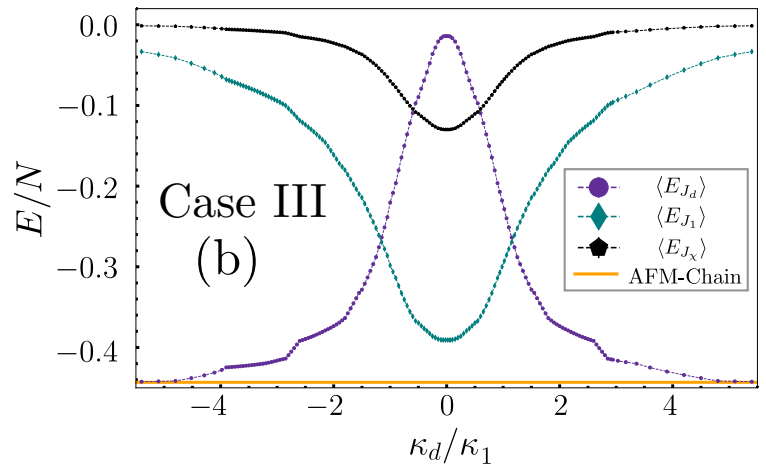
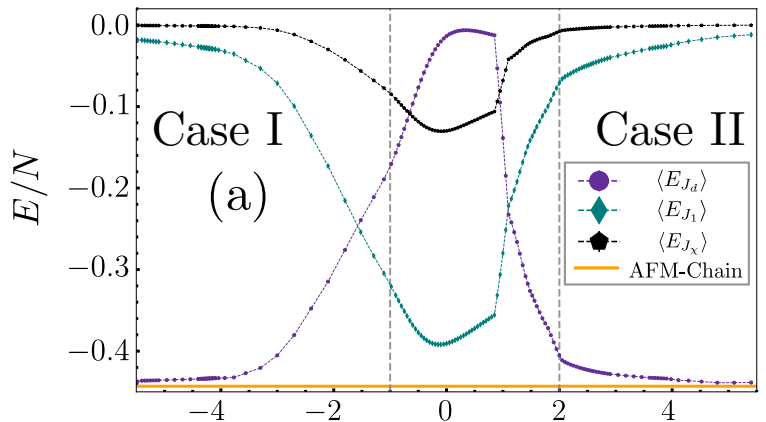
- ◊ Nesting instability of the U(1) CSL to ordered phases (Fermi pockets in $\kappa_d/\kappa_1 > 2$ and E_F crossing);
- ◊ Flattening of central band in $\kappa_d/\kappa_1 \approx -1$ (Case I).

Krüger and Janssen,
Phys. Rev. B 104, 165133
(2021)

$$\kappa_d/\kappa_1 \in [-1, 2]$$

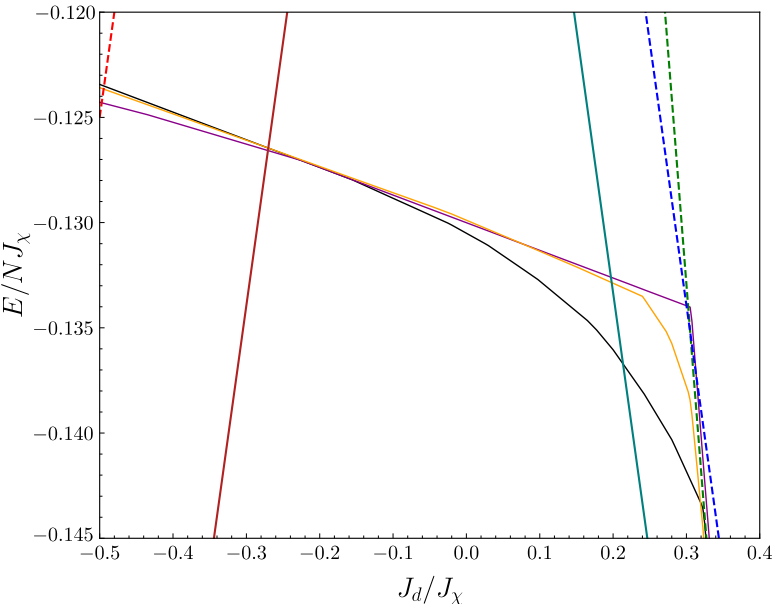


Ground state energy (VMC)

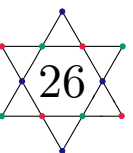


$$E_{AFM} = J_d \left(\frac{1}{4} - \ln(2) \right)$$

$$F(\kappa_d/\kappa_1) = J_1 \langle E_{J_1} \rangle + J_d \langle E_{J_d} \rangle + J_\chi \langle E_{J_\chi} \rangle$$

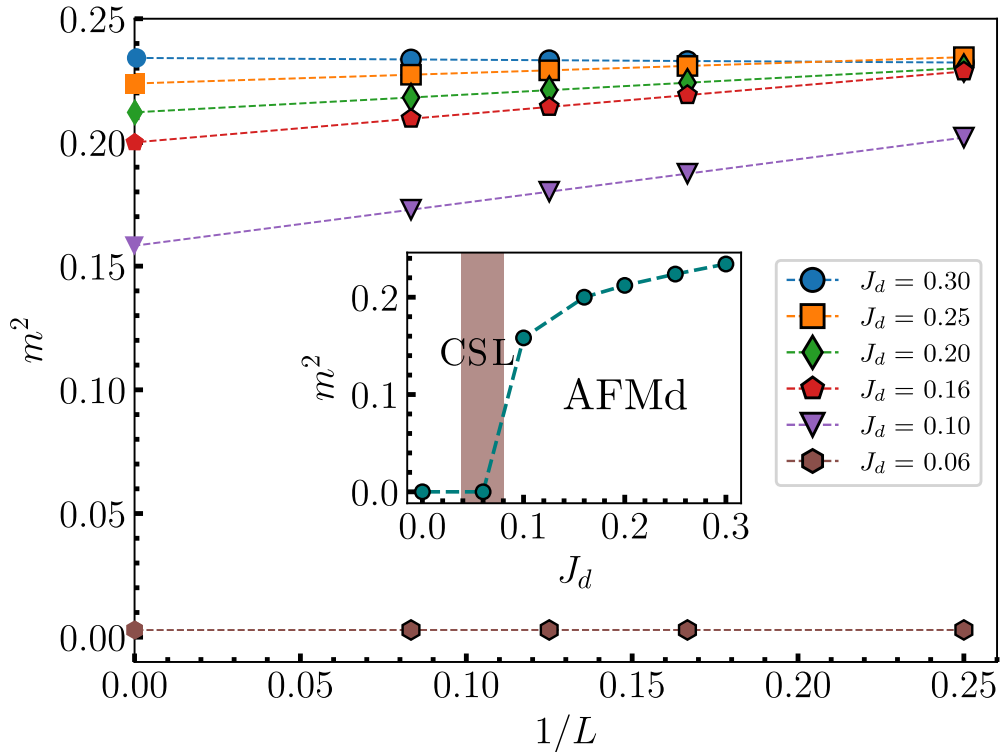


$$J_1 = 0$$



Magnetization and Instabilities

$$(J_1 = -0.01, J_\chi = 1.00)$$

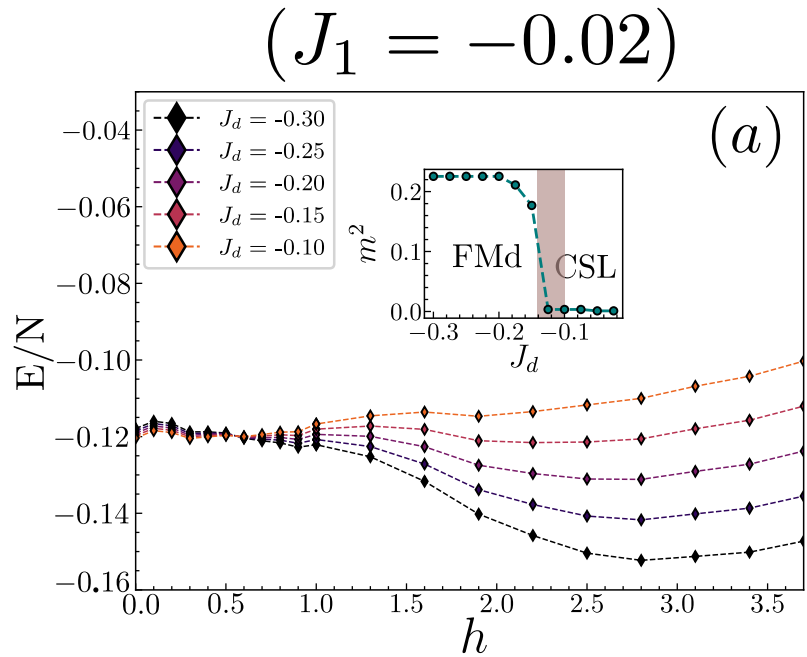
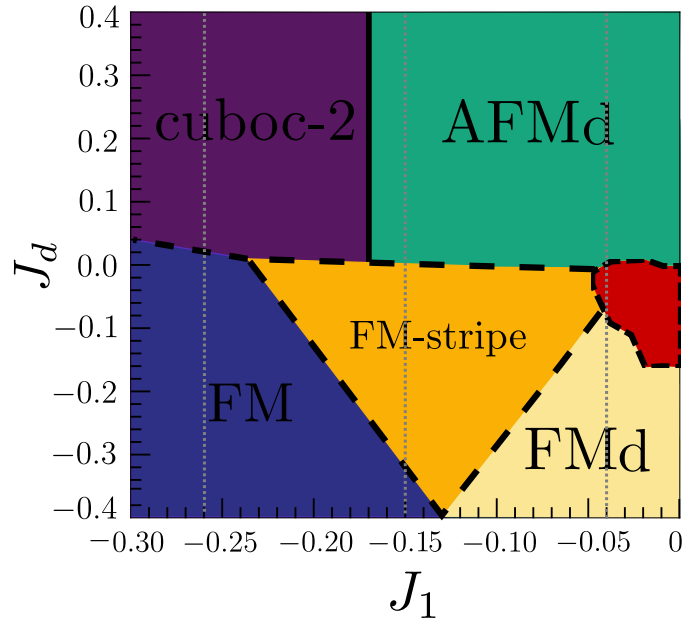


$$\begin{aligned} H_{MFT} = & \sum_{\langle i,j \rangle, \alpha} \chi_{ij} f_{i\alpha}^\dagger f_{j\alpha} + \\ & + h \sum_i \mathbf{m}_i \cdot \mathbf{S}_i \end{aligned}$$

$$m^2 = \lim_{|i-j| \rightarrow \infty} \langle \mathbf{S}_i \cdot \mathbf{S}_j \rangle$$

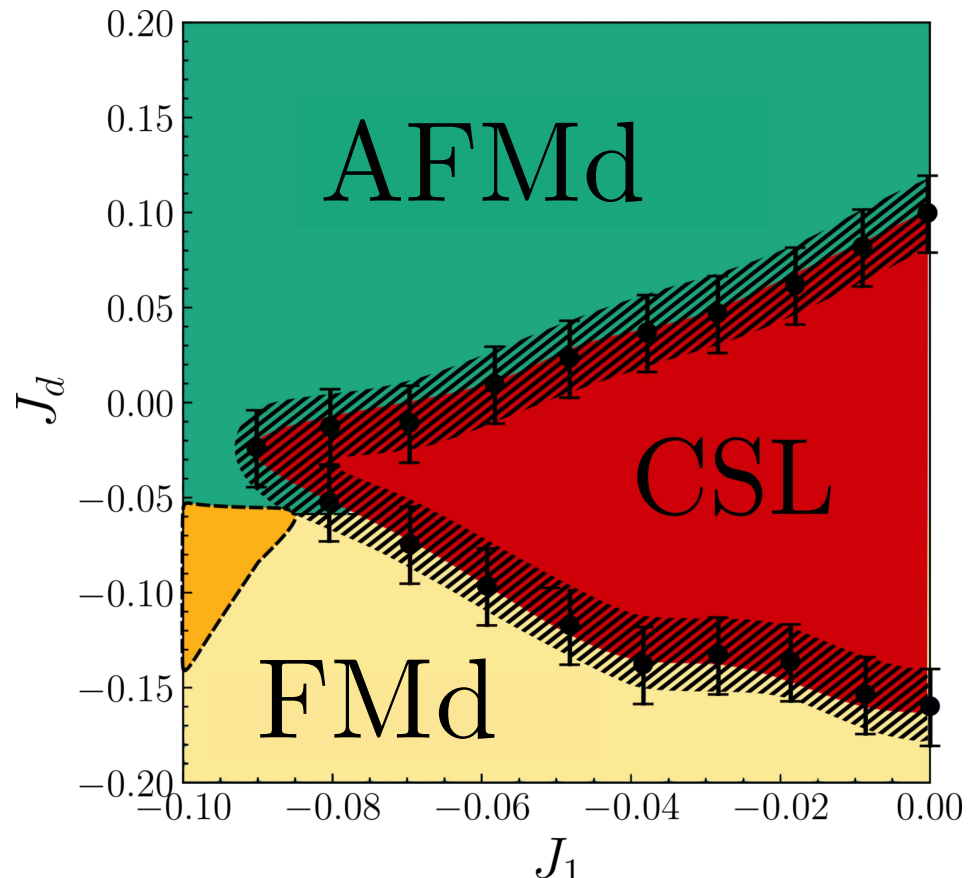
- ◊ SDW ansatz;
- ◊ Finite-size scaling.

Transition between CSL and ordered phases



✳ Phases with $h \neq 0$ are adiabatically connected to the ordered phases.

VMC results near the CSL



Conclusions and outlook

- ◊ New ordered phases: FMd, AFMd, FM-stripe;
- ◊ Continuous phase transition between phases cuboc-1, cuboc-2, octahedral e AFMd;
- ◊ Classically disordered region extended -> Competitive CSL in the phase diagram;

Main ref: (arXiv:2112.03327)

- ◊ AFMd and connection to other ordered phases?
Mondal et al, Jour. of Phys.: Cond. Mat. 33 (50), 505801 (2021)
- ◊ Thermal evolution of ordered phases AFMd, FMd and FM-stripe (Order by disorder)?
Pitts et al, arXiv:2110.11427 (2021)
- ◊ Nature of quantum phase transitions to the GCSL?
Wietek and Läuchli, Phys. Rev. B 95, 035141 (2016) | Hickey et al, Phys. Rev. B 96, 115115 (2017) | Bose et al, arXiv:2204.10329 (2022)

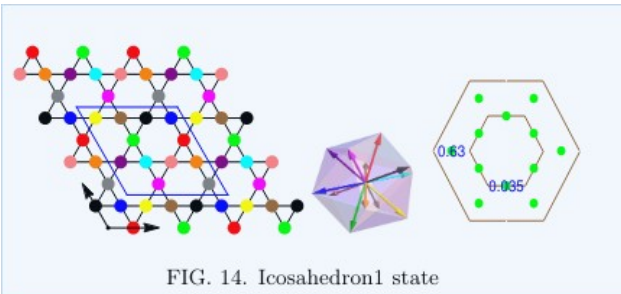
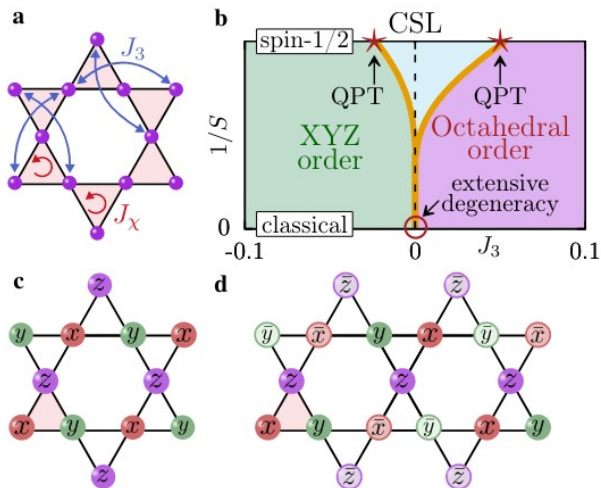


FIG. 14. Icosahedron1 state



Acknowledgements

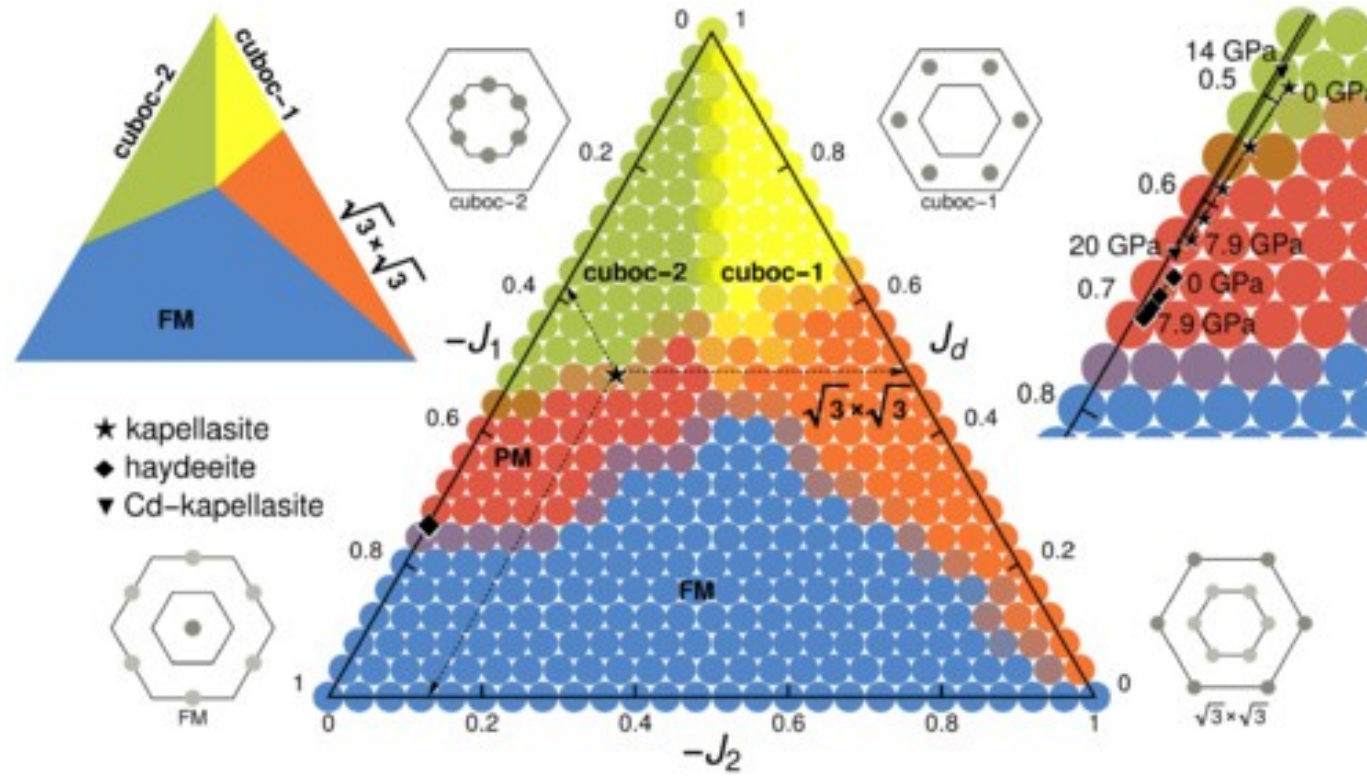


- ✉ Prof. Mathias S. Scheurer.
- ✉ Prof. Eric de Castro e Andrade.
- ✉ Prof. Rodrigo G. Pereira e Fabrizio G. Oliviero.
- ✉ Vitor Dantas Meireles.
- ✉ CAPES - Finance Code 001, via Grant No. 88887.474253/2020-00.

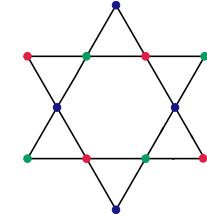


Extra slides

Quantum phase diagram of the J₁-J₂ Heis. model



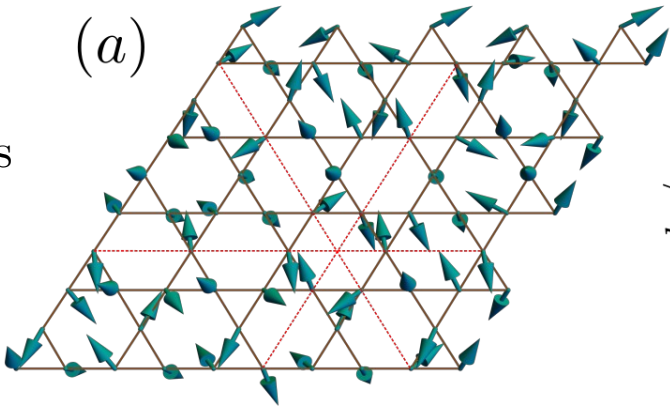
Iqbal *et al*, Phys.
Rev. B 92,
220404(2015)



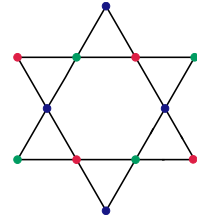
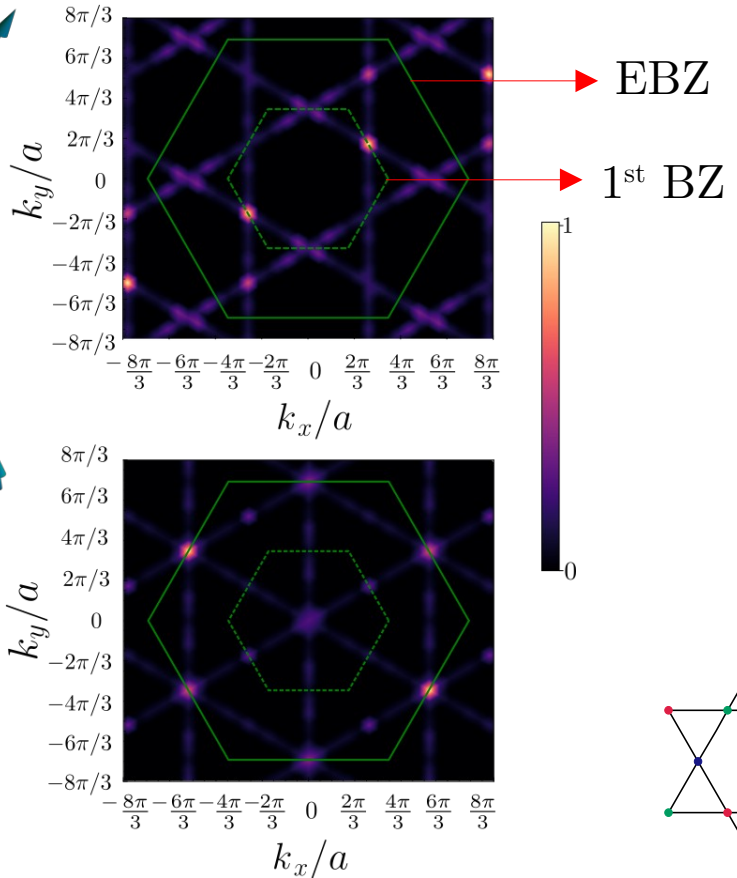
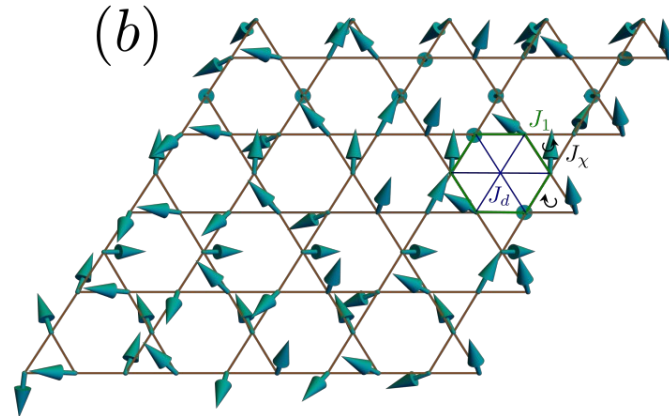
Benchmark: (A)FM chains weakly coupled

$$(J_d \gg J_\chi)$$

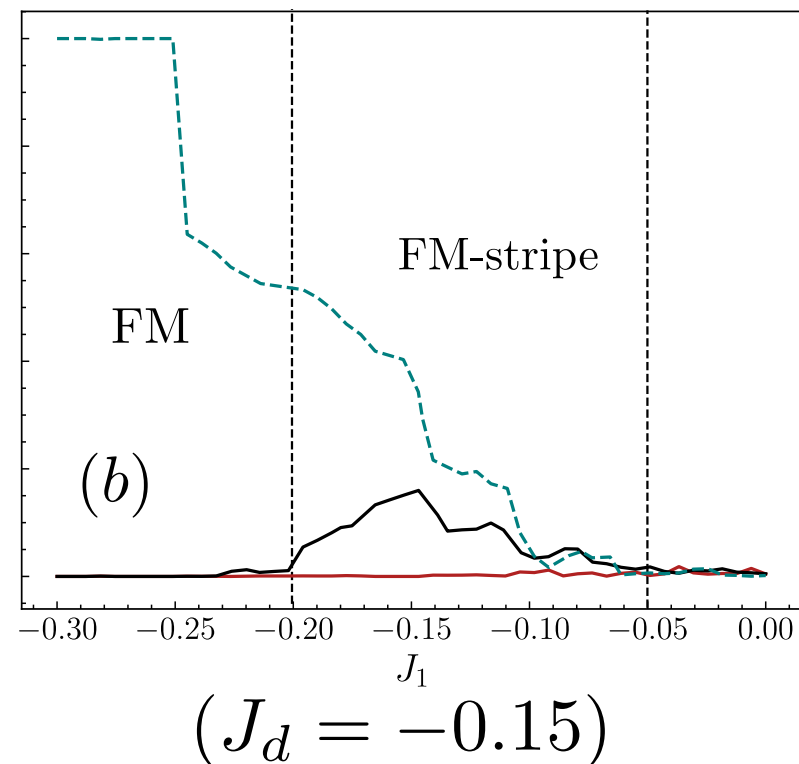
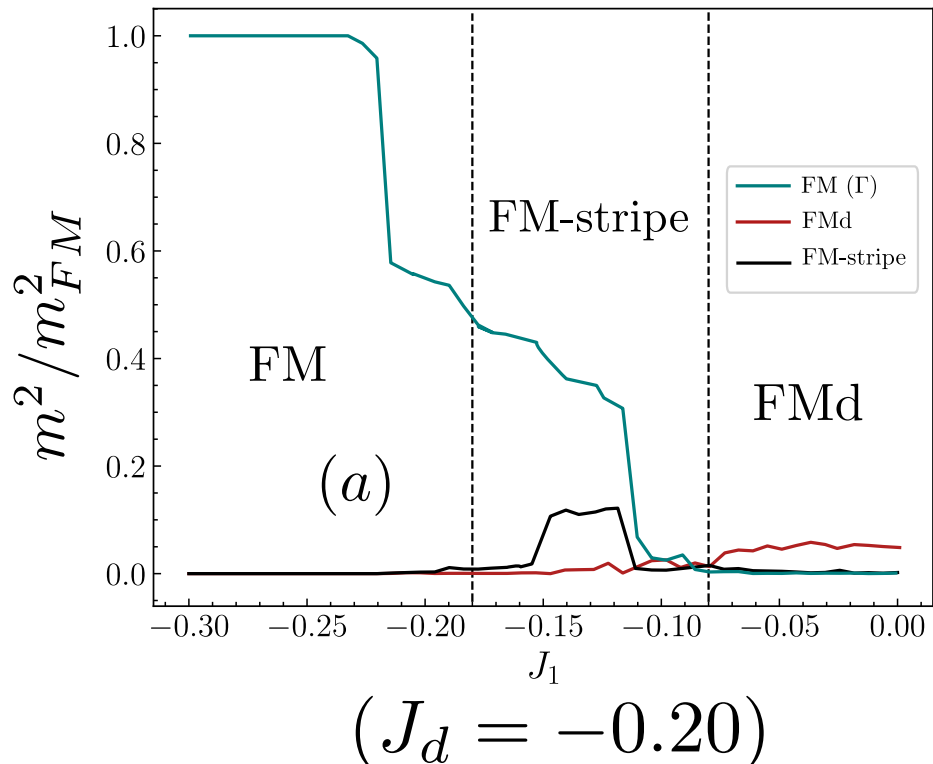
AFM Chains



FM Chains



FM, FM-stripe, FMd phase transition



Shermann Morisson e Matrix Determinant Lemma

Algorithm 3 Variational Monte Carlo

1. Start with a random configuration in \mathbb{A}_α , with $n_\uparrow = n_\downarrow$ in random positions. Store both inverse matrices and save a backup of each initial configuration.
2. Select a new configuration by randomly exchanging the position of two opposite spins. If the new spin is in the k -th column

$$\det \mathbb{A}_\beta = \left(1 + e_k^T \mathbb{A}_\alpha^{-1} u_k \right) \det \mathbb{A}_\alpha \quad (2.61)$$

and

$$\mathbb{A}_\beta^{-1} = \mathbb{A}_\alpha^{-1} - \frac{\mathbb{A}_\alpha^{-1} u_k e_k^T \mathbb{A}_\alpha^{-1}}{1 + e_k^T \mathbb{A}_\alpha^{-1} u_k}, \quad (2.62)$$

with $u_i = [\mathbb{A}_\beta]_{ik} - [\mathbb{A}_\alpha]_{ik}$.

3. Accept or reject the new configuration by the Metropolis rule

$$T(\alpha \rightarrow \beta) = \min \left[1, \frac{p(\beta)}{p(\alpha)} \right] = \begin{cases} \frac{p(\beta)}{p(\alpha)}, & \frac{p(\beta)}{p(\alpha)} < 1 \\ 1, & \frac{p(\beta)}{p(\alpha)} \geq 1 \end{cases}. \quad (2.63)$$

where $\frac{p(\beta)}{p(\alpha)} = \frac{|\langle \beta | \psi \rangle|^2}{|\langle \alpha | \psi \rangle|^2} = \left| \frac{\det \mathbb{A}_\beta}{\det \mathbb{A}_\alpha} \right|^2 = \left(1 + u_k \mathbb{A}_\alpha^{-1} e_k^T \right) \left(1 + u_k \mathbb{A}_\alpha^{-1} e_k^T \right)^*$. This equation only states a minimization of energy. To properly introduce a Metropolis Algorithm one should sort a random number $r \in [0, 1]$: if $r < p(\beta)/p(\alpha)$ the new configuration can still be accepted. Otherwise, if $r \geq p(\beta)/p(\alpha)$, the old configuration is maintained.

4. Go back to step 2 and repeat the algorithm for the desired MC sweeps (one MC sweep is equivalent to N spin exchange attempts).
-

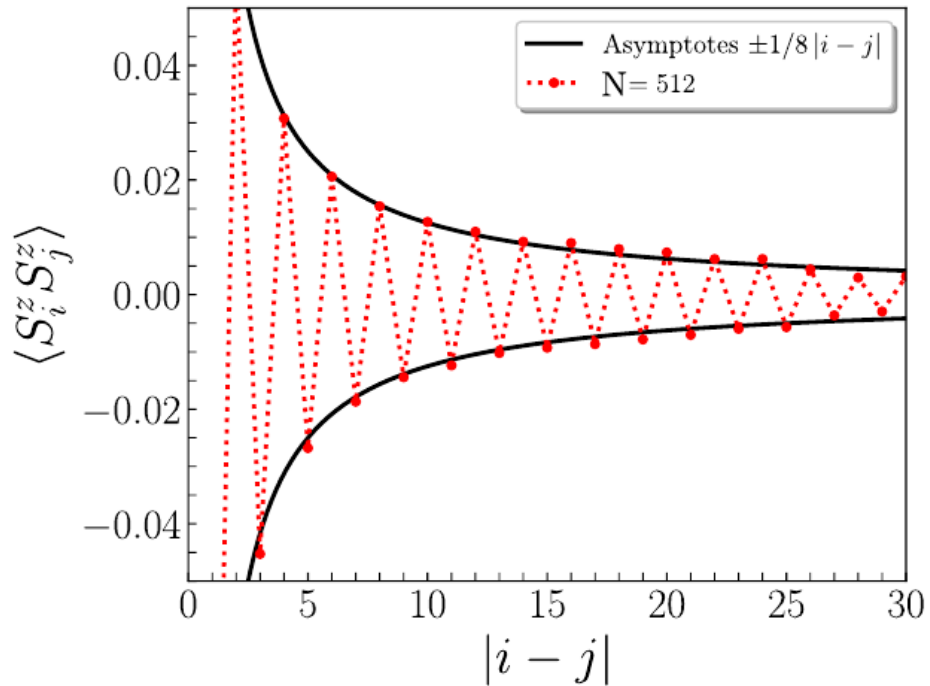
Haldane-Shastry / AFM Heisenberg Chain

N	$E/JN_{(NL)}$	$E/JN_{(L)}$
32	-0.44303 (5)	-0.4435 (4)
64	-0.44232 (5)	-0.4418 (4)
96	-0.44219 (5)	-0.4423 (3)
128	-0.44213 (5)	-0.4419 (3)
256	-0.44212 (5)	-0.4405 (3)
512	-0.44211 (4)	-0.4410 (3)

Source: By the author.

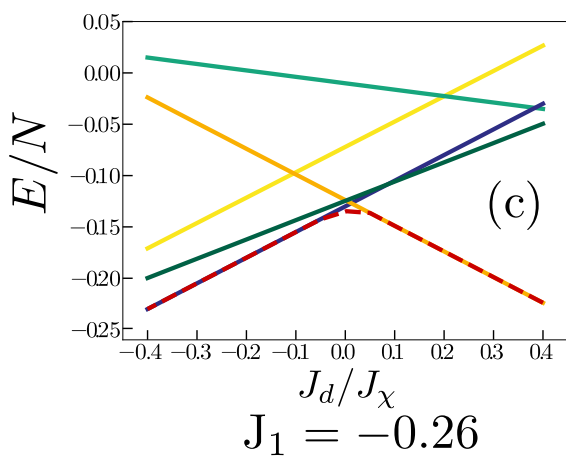
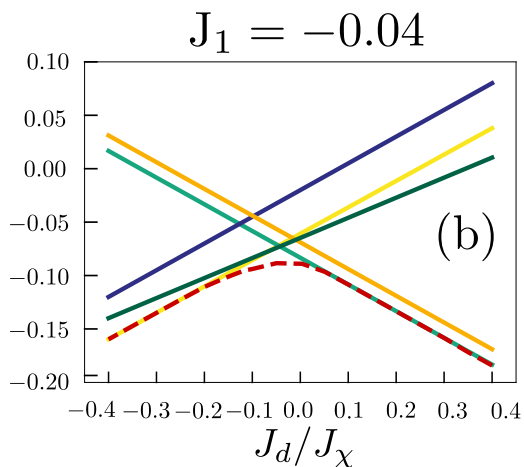
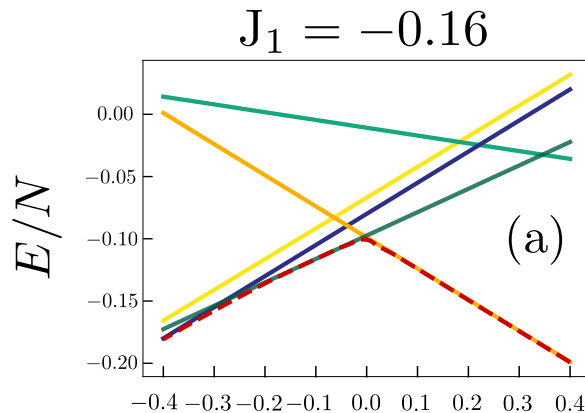
N	E_{HS}^0/JN	E_0/JN
32	-0.413 241 492	-0.413 241 492 (3)
64	-0.411 735 510	-0.411 735 510 (2)
96	-0.411 456 625	-0.411 456 625 (2)
128	-0.411 359 015	-0.411 359 015 (2)
256	-0.411 264 891	-0.411 264 891 (2)
512	-0.411 241 360	-0.411 241 358 (2)

Source: By the author.

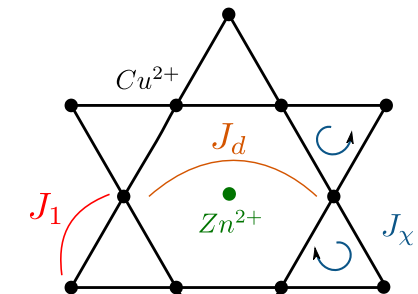


$$\mathcal{H}_{HS} = \sum_{p < q} \frac{J\pi^2 \mathbf{S}_p \cdot \mathbf{S}_q}{N^2 \sin^2 \frac{\pi}{N} (p - q)} = \frac{1}{2} \sum_{p=1}^N \sum_{q=1}^{N-1} \frac{J\pi^2 \mathbf{S}_p \cdot \mathbf{S}_q}{N^2 \sin^2 \frac{\pi}{N} (p - q)}$$

Classical phase diagram for the $J_1 - J_d - J_\chi$ model



- FMd
- AFMd
- FM
- cuboc-2
- FM-stripe
- - - GD minimization



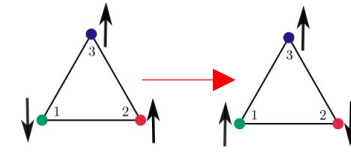
$$H = H_0 + H_\chi$$

$$H_0 = J_{ij} \sum_{\langle i,j \rangle} \mathbf{S}(\mathbf{r}_i) \cdot \mathbf{S}(\mathbf{r}_j)$$

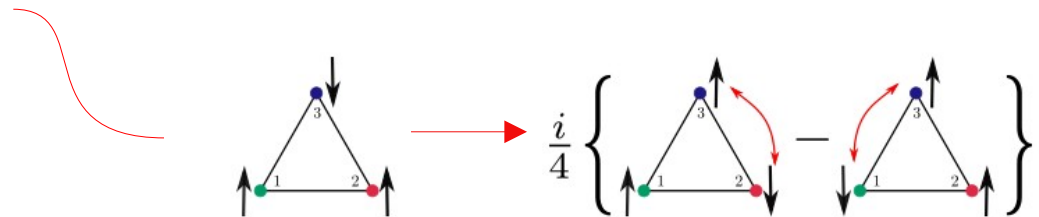
$$H_\chi = J_\chi \sum_{ijk \in \Delta \nabla} \mathbf{S}(\mathbf{r}_i) \cdot [\mathbf{S}(\mathbf{r}_j) \times \mathbf{S}(\mathbf{r}_k)]$$

$J_1 < 0$ (FM), $J_d > 0$ (AFM) e $J_\chi > 0$

Parton Construction and VMC



$$\begin{aligned}
 H = & \frac{1}{2} \sum_{\langle i,j \rangle} J_1 \left\{ \frac{1}{2} \left(f_{i\uparrow}^\dagger f_{i\downarrow} f_{j\downarrow}^\dagger f_{j\uparrow} + f_{i\downarrow}^\dagger f_{i\uparrow} f_{j\uparrow}^\dagger f_{j\downarrow} \right) + \left[\frac{1}{4} - \frac{1}{2} \left(f_{i\uparrow}^\dagger f_{i\uparrow} + f_{j\uparrow}^\dagger f_{j\uparrow} \right) + n_{i\uparrow} n_{j\uparrow} \right] \right\} + \\
 & + \frac{1}{2} \sum_{i,j \in \square} J_d \left\{ \frac{1}{2} \left(f_{i\uparrow}^\dagger f_{i\downarrow} f_{j\downarrow}^\dagger f_{j\uparrow} + f_{i\downarrow}^\dagger f_{i\uparrow} f_{j\uparrow}^\dagger f_{j\downarrow} \right) + \left[\frac{1}{4} - \frac{1}{2} \left(f_{i\uparrow}^\dagger f_{i\uparrow} + f_{j\uparrow}^\dagger f_{j\uparrow} \right) + n_{i\uparrow} n_{j\uparrow} \right] \right\} + \\
 & + J_\chi \frac{i}{4} \left(\sum_{i \neq j \neq k \in \Delta}^3 \varepsilon_{ijk} f_{i\uparrow}^\dagger f_{j\uparrow} f_{j\downarrow}^\dagger f_{i\downarrow} (n_{k\downarrow} - n_{k\uparrow}) - \sum_{i \neq j \neq k \in \nabla}^3 \varepsilon_{ijk} f_{i\uparrow}^\dagger f_{j\uparrow} f_{j\downarrow}^\dagger f_{i\downarrow} (n_{k\downarrow} - n_{k\uparrow}) \right)
 \end{aligned}$$



$$\frac{i}{4} \left\{ f_{3\uparrow}^\dagger f_{2\uparrow} f_{2\downarrow}^\dagger f_{3\downarrow} n_{1\uparrow} + \right. \\
 \left. - f_{3\uparrow}^\dagger f_{1\uparrow} f_{1\downarrow}^\dagger f_{3\downarrow} n_{2\uparrow} \right\}$$

Parton Construction and Gutzwiller Projection

$$\chi_{i,j} \rightarrow \bar{\chi}_{i,j} e^{-ia_{i,j}}$$



$$f_{i,\sigma} \rightarrow e^{i\theta_i} f_{i,\sigma}$$

$$a_{i,j} \rightarrow a_{i,j} + \theta_i - \theta_j$$

MFT ansatz

^{*} Spinons coupled through a U(1) gauge field

Table 1 – Some examples of quantum spin liquids with their respective mean field theories, and possible low energy physics and excitations. For more examples see SAVARY *et al.*⁷ and ZHOU *et al.*⁸

Wen, Physical
Review B
65.16 (2002):
165113.

Lucile Savary
and Leon
Balents (2017)
Rep. Prog.
Phys. 80
016502

	Mean Field Theory	Low energy & excitations
Superconductor	$\mathcal{H}_{MFT} = \sum_{ij} (f_i^\dagger f_j + \Delta_{ij} f_i^\dagger f_j^\dagger + \text{h.c.})$	Topological QSL. Z_2 QSL Anyons, RVB
Semiconductor	$\mathcal{H}_{MFT} = \sum_i \varepsilon_i f_i^\dagger f_i +$ $+ \sum_{ij} (t_{ij} e^{ia_{ij}} f_i^\dagger f_j + \text{h.c.})$	U(1) QSL Gapless photons
Semi-metal	$\mathcal{H}_{MFT} = \sum_{ij} (\tilde{t}_{ij} f_i^\dagger f_j + \text{h.c.})$	U(1) QSL. Algebraic QSLs Dirac Fermions
Metal	$\mathcal{H}_{MFT} = \sum_{ij} (t_{ij} f_i^\dagger f_j + \text{h.c.})$	U(1) QSL. Spinon Fermi Surface

Source: Adapted from SAVARY *et al.*⁷